Plant Physiol. (1997) 113: 1059–1069

Extracellular Matrix Assembly in Diatoms (Bacillariophyceae)[1]

I. A Model of Adhesives Based on Chemical Characterization and Localization of Polysaccharides from the Marine Diatom *Achnanthes longipes* and Other Diatoms

Brandon A. Wustman, Michael R. Gretz*, and Kyle D. Hoagland

Department of Biological Sciences, Michigan Technological University, Houghton, Michigan 49931–1295 (B.A.W., M.R.G.); and Department of Forestry, Fisheries, and Wildlife, University of Nebraska, Lincoln, Nebraska 68583 (K.D.H.)

Extracellular adhesives from the diatoms *Achnanthes longipes*, *Amphora coffeaeformis*, *Cymbella cistula*, and *Cymbella mexicana* were characterized by monosaccharide and methylation analysis, lectin-fluorescein isothiocyanate localization, and cytochemical staining. Polysaccharide was the major component of adhesives formed during cell motility, synthesis of a basal pad, and/or production of a highly organized shaft. Hot water-insoluble/hot 0.5 M $NaHCO_3$-soluble anionic polysaccharides from *A. longipes* and *A. coffeaeformis* adhesives were primarily composed of galactosyl (64–70%) and fucosyl (32–42%) residues. In *A. longipes* polymers, 2,3-, *t*-, 3-, and 4-linked/substituted galactosyl, *t*-, 3-, 4-, and 2-linked fucosyl, and *t*- and 2-linked glucuronic acid residues predominated. Adhesive polysaccharides from *C. cistula* were EDTA-soluble, sulfated, consisted of 83% galactosyl (4-, 4,6-, and 3,4-linked/substituted) and 13% xylosyl (*t*-, $4_f/5_p$-, and 3_p-linked/substituted) residues, and contained no uronosyl residues. *Ulex europaeus* agglutinin uniformly localized α(1,2)-L-fucose units in *C. cistula* and *Achnanthes* adhesives formed during motility and in the pads of *A. longipes*. D-Galactose residues were localized throughout the shafts of *C. cistula* and capsules of *A. coffeaeformis*. D-Mannose and/or D-glucose, D-galactose, and α(*t*)-L-fucose residues were uniformly localized in the outer layers of *A. longipes* shafts by *Cancavalia ensiformis*, *Abrus precatorius*, and *Lotus tetragonolobus* agglutinin, respectively. A model for diatom cell adhesive structure was developed from chemical characterization, localization, and microscopic observation of extracellular adhesive components formed during the diatom cell-attachment process.

Achnanthes longipes, *Cymbella cistula*, *Cymbella mexicana*, and *Amphora coffeaeformis* are relatively large, fast-growing, unicellular organisms specialized in cell motility and attachment via distinct extracellular structures. These adhesive structures can be easily manipulated, observed, and isolated for the study of synthesis, transport, modification, and assembly of extracellular polymers. Modeling such systems can provide a better understanding of how plant cells adhere to surfaces and interact with their surrounding environments. Furthermore, these diatoms are a major component of marine and freshwater biofilms (Round et al., 1990) and thus cause a variety of biofouling problems (Alberte et al., 1992). Understanding how these cells adhere to surfaces will also aid in the development of new antibiofouling surfaces and of adhesives for use in marine and freshwater environments.

Most diatoms attach to surfaces via polymers excreted from a slit (raphe) or apical pore field in the siliceous cell wall (frustule) (Hoagland et al., 1993). Exuded polymers are assembled into a variety of structures, such as trails (material left behind during motility), sheaths (organic matrices tightly associated with the cell wall), capsules (organic matrices loosely associated with the cell walls), and stalks (permanent attachment structures) (Hoagland et al., 1993). Stalks consist of three regions: (a) a surface-adhered pad; (b) a collar associated with the frustule at a terminal nodule or apical pore field; and (c) an intervening shaft that separates the cell from the surface (Daniel et al., 1987; Wang et al., 1997). Previous studies indicate that diatom ECM consists primarily of polysaccharides, although protein has been previously identified in *Berkeleya rutilans* and lipids have not yet been detected in any diatom extracellular structures (Hoagland et al., 1993).

[1] This research was supported by the Office of Naval Research (grants N00014-91-J-1108, N00014-94-1-0273, and N00014-94-1-0766 to M.R.G. and K.D.H.) and a Michigan Technological University Fellowship Award to B.A.W. This is journal series no. 11683 of the Agricultural Research Division at the University of Nebraska. This work represents a portion of a dissertation by B.A.W. to be submitted as partial fulfillment for the doctor of philosophy degree from the Department of Biological Sciences, Michigan Technological University, Houghton.

* Corresponding author; e-mail mrgretz@mtu.edu; fax 1–906–487–3167.

Abbreviations: APA, *Abrus precatorius* agglutinin; CMC, 1-cyclohexyl-3-(2-morpholinoethyl)carbodiimide-metho-*p*-toluenesulfonate; CPC, cetylpyridinium chloride; DAPI, 4′,6-diamidino-2-phenylindole; DIC, differential interference contrast; ECM, extracellular matrix; FITC, fluorescein isothiocyanate; F/2, F/2 enriched seawater culture medium; GSII, *Griffonia simplicifolia* agglutinin; Gul, gulose; LTA, *Lotus tetragonolobus* agglutinin; MIS, mechanically isolated stalks; PSA, *Pisum sativum* agglutinin; UEA I, *Ulex europaeus* agglutinin; VFA, *Vicia faba* agglutinin; WIBS, hot water-insoluble/hot bicarbonate-soluble fraction; WS, hot water-soluble fraction.

Microscopic observations of the marine diatom *A. longipes* revealed two modes of initial attachment, passive and active (Wang et al., 1997). The active mode requires de novo secretion of ECM polymers, whereas passive attachment of *A. longipes* appears to involve mainly hydrophobic interactions with existing cell surface polymers (Wang et al., 1997). Once the cells have attached to a surface they exhibit both adnate and pedunculate habits. *A. longipes* cells spread out evenly on a glass surface before producing more permanent attachment structures in the form of stalks (Hoagland et al., 1993; Wang, 1995).

Daniel et al. (1987) demonstrated that whole stalks of *A. longipes, Licmophora flabellata,* and *Licmophora abbreviata,* as well as the ECM of *A. coffeaeformis* (Daniel et al., 1980), did not always stain uniformly, providing evidence for chemically unique regions. Stains, however, can be relatively nonspecific and provide only an indication of the presence or absence of anionic groups, neutral carbohydrates, proteins, and lipids. Although past studies presume that diatom extracellular structures are composed mostly of highly branched, complex carbohydrate polymers, few studies have centered on the characterization and localization of specific units and polymers within the ECM. The use of specific probes, combined with detailed fractionation and chemical characterization procedures, furthers the understanding of properties such as flexibility, gelling, resistance to desiccation, and adhesion to surfaces. We report here a chemical characterization of extracellular polymers of several diatoms and localization of these polymers with fluorescent lectin conjugates and specialized stains during various stages of development.

MATERIALS AND METHODS

Culturing Conditions and Source of Algal Material

Unialgal cultures of the marine diatoms *Achnanthes longipes* Ag. (no. 330) and *Amphora coffeaeformis* Ag. Kütz. (no. 2080) were obtained from the National Institute for Environmental Studies collection and the University of Texas Culture Collection, respectively, and were cultured in sterile F/2-enriched sea water (Guillard, 1975). Freshwater *Cymbella cistula* (Ehr.) Kirchn. and *Cymbella mexicana* (Ehr.) Cl. were isolated from nature into a unialgal culture in sterile WC and soil water (Pringsheim, 1946), respectively. All cultures were incubated at 18°C with a 12-h:12-h light: dark cycle (100 μmol m^{-2} s^{-1}) for 2 to 3 weeks. To reduce bacterial contamination, *A. longipes* inoculum was briefly blended at low speed, washed repeatedly, and treated with a mixture of kanamycin, erythromycin, and penicillin-G (30 μg/mL each) in filtered, sterilized F/2. If *A. longipes* was kept in static culture longer than 3 weeks, cells produced large amounts of capsular material. In cultures of all ages, some floating colonies were present. To isolate substrate-associated cells and ECM, we harvested 2- to 3-week-old cultures of *A. longipes, A. coffeaeformis, C. cistula,* and *C. mexicana.* We first removed floating colonies by pouring off culture medium and then dislodged attached cells and associated ECM by scraping with a spatula.

Mechanical Isolation and Chemical Fractionation of Diatom ECM

Stalks were mechanically isolated from *A. longipes, C. cistula,* and *C. mexicana* by homogenization for 30 min in 0.05 M Tris (pH 8.0; containing 0.4 M NaCl for *A. longipes*) at 5°C, filtration on Nitex mesh (Aquatic Research Instruments; 25-μm mesh for *A. longipes;* 64-μm mesh for *C. cistula* and *C. mexicana*), followed by rinsing on Nitex with distilled water. MIS collected from Nitex were microscopically examined and clean preparations were lyophilized and stored.

MIS of *A. longipes* and *C. cistula* were chemically fractionated by defatting with 90% (v/v) ethanol at 23°C for 10 min with four repetitions, followed by three extractions with 0.5 M $NaHCO_3$ for 1 h at 95°C, and, finally, one extraction with water for 1 h at 95°C. Aqueous extracts were combined and precipitated with 2% (w/v) CPC. The CPC precipitate was decomplexed overnight in saturated sodium acetate in 95% (v/v) ethanol, washed several times with 95% (v/v) ethanol, and lyophilized. CPC-soluble polymers were dialyzed overnight against distilled water at 5°C and freeze-dried. *A. longipes* CPC-insoluble material accounted for 70% (w/w) and CPC-soluble polymers accounted for 3% (w/w) of the MIS preparation. Hot aqueous insoluble material was washed with distilled water and lyophilized. *A. longipes* insoluble residue was primarily frustules and represented 14% (w/w) of the original MIS.

Mucilage capsules of *A. coffeaeformis* were separated from cells by passage through a 23-gauge followed by an 18-gauge needle. The resulting suspension was filtered with an 8-μm polycarbonate filter (Nucleopore, Corning Costar Corp., Cambridge, MA) and the filtrate dialyzed for 3 d against distilled water at 5°C and freeze-dried.

Chemical Isolation of Diatom Adhesives

In addition to mechanical isolation methods, chemical procedures were developed for more efficient isolation of adhesive polymers. Cells and associated ECM of *A. longipes, A. coffeaeformis,* and *C. cistula* were centrifuged at 700*g* for 5 min and washed several times with distilled water. The pellet was extracted three to five times with 90% ethanol for 10 min at 22°C with centrifugation at 700*g* for 5 min after each extraction. The defatted pellet was washed three times with distilled water and extracted for 1 h with 90°C distilled water to remove WS material. The pellet was then extracted with 95°C 0.5 M $NaHCO_3$ to yield a WIBS fraction, or with 0.2 M EDTA (pH 7.0) at 22°C for 30 min for *C. cistula.* EDTA-soluble polymers were first dialyzed against 0.5 M imidazole (pH 7.0) overnight at 5°C, and then overnight against distilled water and freeze-dried. WS and WIBS fractions were dialyzed overnight against distilled water and freeze-dried. A portion of the hot $NaHCO_3$-soluble polymers of *A. longipes* was precipitated with 2% (w/v) CPC and purified as described above. The chemical isolation process was monitored by DIC and Alcian blue staining (0.1% [w/v] in 3% [v/v] acetic acid, pH 2.5) as described by Daniel et al. (1987).

CMC-Activated Prereduction of Uronic Acids

To identify and quantify uronic acids in diatom ECM, the prereduction method of Kim and Carpita (1992) for uronic acid-containing polymers was modified to accommodate milligram quantities. Approximately 5 mg of sample was dissolved in 5 mL of distilled water and the pH adjusted to 4.75 with 0.01 N HCl. The activated ester (Taylor and Conrad, 1972) was formed by adding 60 mg of CMC while stirring. A pH of 4.75 was maintained by the addition of HCl. After about 2 h, the pH stabilized, 350 μL of cold 4 M imidazole (pH 7.0) was added, and the mixture was reduced with 35 mg of $NaBD_4$ for 1 h at 5°C with stirring. After the addition of glacial acetic acid (to pH 5.5) to destroy excess $NaBD_4$, the sample was dialyzed for 40 to 50 h against distilled water at 5°C, lyophilized, and weighed in preparation for monosaccharide analysis.

Monosaccharide Analysis

Following hydrolysis with 2 N trifluoroacetic acid for 3 h at 121°C under vacuum, hydrolyzates were reduced with $NaBD_4$ and acetylated (Blakeney et al., 1983). Alditol acetates were separated on a fused silica capillary column (Supelco SP-2330, Bellefonte, PA; 15 m, 0.25 mm i.d., 70 cc/min, 200°C for 3 min, ramped to 240°C at 5°C/min) and detected using a GC-MS system (Magnum, Finnigan-MAT, San Jose, CA). Constituents were identified by their retention times and mass spectra. Quantification was based on response factors derived from repeated injections of standards that had been subjected to the same hydrolytic procedures as the diatom samples (Sloneker, 1972). Prereduced samples containing aldoses corresponding to CMC-reduced uronic acids were quantified by comparison of the mass ion ratio 189/188. The mass ion ratios for hydrolyzates of polygalacturonic acid (0.9), alginic acid (0.88), and pectin (0.86) and the neutral monosaccharide standards Man (0.21), Gal (0.20), and Glc (0.22) were used for calibration. Efficiency of prereduction by the CMC method was determined to be approximately 80% by the carbazole calorimetric assay method (Bitter and Muir, 1962) as described below.

Methylation Analysis

Fractions containing uronosyl residues were treated with Dowex 50W-X12 (H^+ form) prior to per-*O*-methylation (Waeghe et al., 1983) and reduced with 1 M lithium triethylborodeuteride in tetrahydrofuran for 1.5 h at 22°C following per-*O*-methylation (York et al., 1985). Prior to per-*O*-methylation, sulfated polymers were treated as above with Dowex to ion-exchange sulfate groups in preparation for conversion to pyridinium salts (Barker et al., 1984) to enhance solubility in DMSO (Stevenson and Furneaux, 1991). Polymers were per-*O*-methylated with butyllithium in DMSO and methyl iodide (Pas Parente et al., 1985; Kvernheim, 1987), and purification of methylated polymers was accomplished by exhaustive dialysis against running distilled water. Trifluoroacetic acid hydrolysis and reduction were performed according to Waeghe et al. (1983), and acetylation of per-O-methylated alditols was as described by Harris et al. (1984). To allow determination of the linkages of anhydro-sugars, the 4-methylmorpholine-borane method for reductive hydrolysis was used (Stevenson and Furneaux, 1991). Per-O-methylated alditol acetates were separated on a SP-2330 column (30 m, 0.25 mm i.d., 150–245°C at 4°C/min, held at 245°C for 20 min, injector 240°C). Mass spectra were obtained by GC/MS (Finnegan-MAT) operated in the electron-impact mode and used to detect column effluent. Glycosyl linkage/substitution sites were assigned according to characteristic mass ion fragments reported by Jansson et al. (1976) and Waeghe et al. (1983). Darvill et al. (1980) glycosyl linkage/substitution nomenclature is used.

To identify 4-linked gulosyl, alginic acid was prereduced by the CMC method, converting 4-guluronosyl and 4-manuronosyl to 4-Gul and 4-Man. Methylation analysis of prereduced alginic acid revealed peaks for two 4-linked hexoses. One peak correlated with the retention time of a 4-Man derived from a β-1,4-mannan control, and the other peak was assigned as 4-Gul.

^{13}C-NMR Spectroscopy

Proton decoupled ^{13}C-NMR spectra were recorded with a spectrometer (Bruker, Billerica, MA) at 100 MHz on 80 mg of sample in ^2H_2O. Analyses were done at 70°C with a spectral width of 23.8 kHz, a pulse width of 3.0 s, and an acquisition time of 0.688 s. Chemical shifts were measured relative to the internal standard DMSO and converted to values relative to external tetramethylsilane (DMSO = 39.45 ppm).

IR Spectroscopy

Samples were prepared by grinding 100 g of sample with 1 mg of potassium bromide, pressing the mixture to form a pellet, and drying overnight in a desiccator over P_2O_5. A Fourier transform IR spectrometer (model 7000 series, Nicolet, Madison, WI) was used to read absorbances from 580 to 4000 cm^{-1}.

Other Analytical Methods

Uronic acid was determined by the carbazole assay (Bitter and Muir, 1962). Sulfate and protein were determined according to the methods of Craigie et al. (1984) and Lowry et al. (1951), respectively. Amino acid analysis was performed with an automatic derivatizer (model 420A, Applied Biosystems) with an online HPLC separation system (model 130A, Applied Biosystems). Hydrolysis of MIS of *A. longipes* and *C. cistula* was accomplished using 6 N HCl at 110°C for 20 h under vacuum. All amides are detected with this method, together with their corresponding amino acids. Modified amino acids could not be detected by this protocol.

Lectin Labeling

Lectins conjugated with FITC were purchased from Sigma and their reported specificities are listed in Table II. Diatom cells and ECM were isolated from 2-d-old cultures as described above and placed in microcentrifuge tubes for label-

ing. *A. longipes* was washed several times with F/2 and *C. cistula* with PBS (0.01 M PO_4^{-3}, pH 7.0, 0.15 M NaCl) and then incubated for 30 min in 1% (w/v) BSA in F/2 or PBS. Following centrifugation at 500*g* for 2 min, pellets were resuspended in 50 μL of lectin-FITC solution (100 μg/mL in F/2 or PBS, 1% [w/v] BSA, pH 7.0), allowed to incubate for 2 h in the dark at 18°C, and washed five times with F/2 or PBS. A light microscope (Axioskop, Zeiss) equipped for DIC and epifluorescence microscopy with either a broad-emission FITC filter set (Zeiss; 450–490 nm excitation and >520 nm emission filter) or a narrow-emission FITC filter set (Zeiss; 485 nm excitation and 535–540 nm emission) was used. Controls included adding the corresponding monosaccharide and competing off the bound lectin-FITC, or preabsorption of lectin-FITC with a suitable polymer such as cellulose, mannan, or fucoidan (Table II).

Autofluorescence, Birefringence, DAPI, Tinopal, and Ruthenium Red Staining

A. longipes cells and associated mucilage were scraped from 3-d-old cultures and examined for autofluorescence with epifluorescence under a UV filter set (Zeiss; 360 nm excitation and >420 nm emission filter). DAPI (0.1 mg/mL in sea water) or Tinopal (0.05% [w/v] in distilled water) was added to the material on a slide and observed with fluorescence under the above UV filter set. Ruthenium red (0.2% [w/v] in distilled water) was used to stain isolated material, which was then observed by DIC microscopy. Screening for birefringence was accomplished using standard polarization microscopy techniques.

RESULTS

Isolation and Fractionation of Adhesive Polymers

The chemical isolation procedure was generally preferable, since with it we could efficiently isolate large quantities of extracellular polymers and analyses revealed the same polymers in both chemically isolated adhesives and mechanically isolated material. Alcian blue staining of diatom ECM proved useful in monitoring the sequential ECM chemical isolation procedure (Fig. 1, A–D). Defatting with ethanol followed by hot water extraction of *A. longipes* and *C. cistula* did not disrupt adhesion to glass culture vessels. Frustules remained attached to glassware via stalks, and pads and collars remained intact, although much intracellular material was removed (Fig. 1C). *A. longipes* stalks swelled slightly during hot water extraction, especially in the region adjacent to the frustule, and we observed that these same areas contracted considerably upon drying compared with the rest of the stalk. Methylation analysis of the WS fraction (data not shown) indicated that polysaccharides removed with hot water were made up predominantly of 3-linked glucosyl units with smaller amounts of 6-, 2-, and *t*- linked glucosyl units, typical of chrysolaminaran (Darley, 1977). Trace amounts of the dominant glycosyl linkages/substitutions found in *A. longipes* WIBS fractions were also detected in the WS fraction. Microscopic observations with Alcian blue staining revealed no visible substrate-associated ECM following hot 0.5 M $NaHCO_3$ extraction of *A. longipes* and *C. cistula*. *A. longipes* WIBS polymers immediately began to reaggregate upon cooling and further precipitated upon dialysis against distilled water. Monosaccharide analysis of the precipitated polymers revealed a similar sugar distribution as the bulk of the extract, with increased Man being the only exception. When *C. cistula* stalks were treated with 0.2 M EDTA and *trans*-1,2-diaminocyclohexane-*N,N,N',N'*-tetraacetic acid (following hot water extraction) at 23°C, they were completely solublized, whereas *A. longipes* stalks appeared unaffected by this treatment.

A. longipes: Marine Stalk Former

Preliminary analysis of capsular material, floating colony ECM, and attached cell ECM revealed no significant differences in monosaccharide composition (data not shown). The following analyses and localization studies were car-

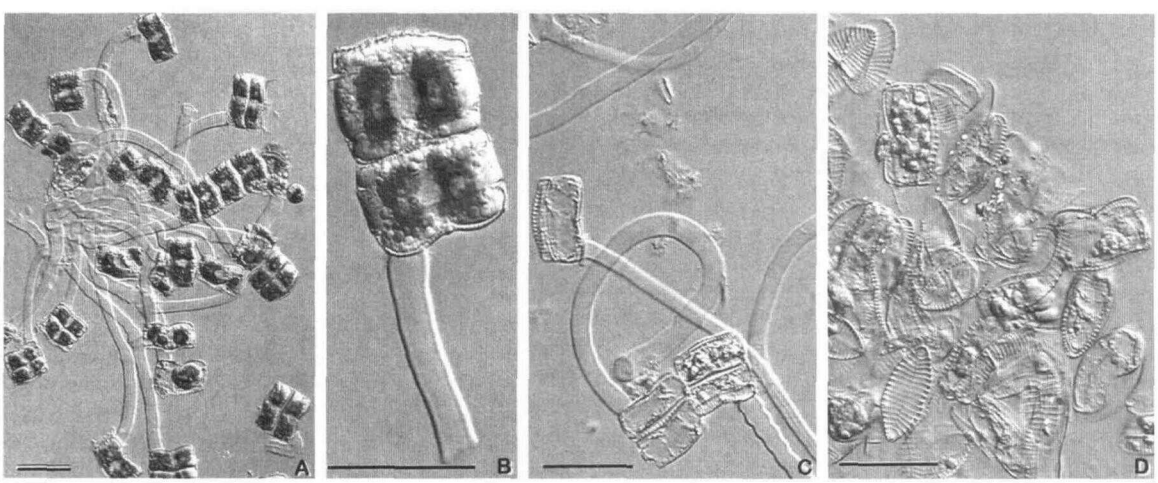

Figure 1. *A. longipes* during chemical isolation of adhesives as visualized with DIC microscopy. A and B, Native culture. C, Material remaining following sequential extraction with 90% ethanol and 90°C water. D, Insoluble residue remaining after extraction with 95°C 0.5 M $NaHCO_3$. Frustules are the major component. Scale bar = 25 μm.

ried out on material derived from attached organisms. MIS from *A. longipes* contained a substantial amount of neutral sugar (40%), uronic acid (10%), and protein (5%). Relative amounts of constituent saccharides in fractions, based on monosaccharide and methylation analysis, are presented in Table I. Monosaccharide analysis of MIS, WIBS/CPC-insoluble, and WIBS/CPC-soluble fractions revealed glucuronosyl residues (GlcUA) and eight different neutral sugar units (Glc, Man, Gal, Gul, Xyl, Ara, Fuc, and Rha). The majority of adhesive polymers were contained in the

Table I. *Glycosyl unit and linkage/substitution site profiles of unfractionated and fractionated extracellular adhesives*

Monosaccharide quantitation was by GC/MS of alditiol acetates and each monosaccharide is presented as a percentage of the total detected. Glycosyl linkage/substitution sites were determined by methylation analysis (GC/MS of partially methylated alditol acetates). Linkage/substitution sites for each residue are listed in order of decreasing relative abundance.

	Glc	GlcUA	Gal	Man	Gul	Xyl	Ara	Fuc	Rha
A. longipes									
MIS[a]	11% 4-	10% *t*-	25%	16% 4-	–[c]	10%	3%	23%	3%
WIBS[b]	3% 3-	ND[d]	28% 2,3- *t*- 3- 4-	8% *t*- 6-	ND 4-	11% *t*- $4_f/5_p$-	–	42% *t*- 3- 4- 2-	8% 2-
WIBS/CPC-insoluble	–	9% *t*- 2-	29% 2,3- 3,6- *t*- 3- 4-	6% *t*- 6-	8% 4-	9% *t*- $4_f/5_p$-	–	33% *t*- 3- 4- 2-	6% 2-
WIBS/CPC-soluble	8% 4- 3-	5%	18% *t*- 4-	11% *t*- 4-	–	11% *t*- $4_f/5_p$-	–	41% *t*- 3- 2,3- 3,4- 2-	6%
Insoluble residue	14%	ND	5%	70%	–	9%	–	3%	–
A. coffeaeformis									
Mechanically isolated[a] capsules[b]	40% 3- *t*- 4- 3,6-	7% 4- *t*- 2,4-	13% 3,6- 3- 6- 3,4-	13% 4,6- 6-	–	9% $4_f/5_p$-	–	9% *t*- 4- 3- 2- 2,3-	9% 2,3-
WS[b]	20%	ND	26%	3%	–	8%	2%	31%	8%
WIBS[b]	5%	ND	32%	5%	–	13%	–	32%	13%
C. cistula									
MIS[a]	4% 4- *t*-	–	69% 3,4,6- 4,6- 3,4- 4- 3-	3%	–	18% *t*- $4_f/5_p$-	1% *t*-	–	2% 2,4-
EDTA-soluble	1%	–	83% 4- 4,6- 3,4-	–	–	13% *t*- $4_f/5_p$- 3-	–	1%	–
Insoluble residue[a]			4-	4-		$4_f/5_p$-			2,4-
C. mexicana									
MIS[a]	5%	1%	57% 4-	12% 4- 4,6-	–	16% $4_f/5_p$-	1%	2%	6%

[a] Results indicate that polysaccharides from MIS, capsules, and insoluble residues were undermethylated, thus fewer linkage/substitution sites could be confidently identified. [b] A methylated hexosyl residue was also detected as a minor component by monosaccharide analysis. [c] –, Not found. [d] ND, Not determined.

WIBS fraction and consisted of 42% fucosyl residues (*t*-; 3-; 4-; 2-; 3,4-; and 2,3-linked/substituted) and 28% galactosyl units (2,3-; *t*-; 4-; 3,6-; 4,6-; and 6-linked/substituted). 4-Linked gulosyl residues were detected only in the WIBS/CPC-insoluble fraction. Glc was not detected in the WIBS/CPC-insoluble fraction by monosaccharide analysis; however, small amounts of 3-, 4-, and *t*-Glc were detected by methylation analysis. Multiple linkage/substitution patterns were revealed for Xyl, Rha, Man, and GlcUA in both CPC-soluble and CPC-insoluble WIBS fractions. Man (70%) was the major constituent of the MIS-insoluble residue, with lesser amounts of Glc (14%), Xyl (9%), Gal (5%), and Fuc (3%) (determination of uronosyl units was not done for this sample) (Table I).

^{13}C-NMR of the WIBS/CPC-insoluble fraction revealed five resonances in the anomeric carbon region (90–110 parts per million), including a C-1 shift corresponding to a furanose conformation (110 parts per million), two resonances tentatively assigned to C-6 of 6-deoxy sugars (approximately 15 parts per million), and an indication of uronic acid carbonyl carbon (175 parts per million). Further NMR analysis was hindered by the high viscosity and complexity of the polymer(s). More detailed NMR analysis will require separation of constituent polymers and/or partial hydrolysis and analysis of oligosaccharides. The sulfate content of the MIS/$NaHCO_3$-soluble/CPC-insoluble fraction was 5.6%, and IR analysis of the same fraction yielded a substantial peak at approximately 1240 cm^{-1}, indicating the presence of sulfate ester (Craigie and Leigh, 1978). A diagrammatic representation of attachment structures and a summary of lectin labeling patterns for *A. longipes* are presented in Figure 2 and Table II, respectively. Application of LTA-FITC (Fig. 3C) and APA-FITC yielded an intense fluorescence of pads and collars and less intensity in the shaft region. LTA-FITC was also localized between frustules (Fig. 3E) and APA-FITC-labeled gamete-encapsulating matrices. ConA-FITC bound intensely to pads, shafts, collars, and immature valves (Fig. 3, G and H). UEA-FITC selectively bound trails, pads, collars, and between mature frustules (Fig. 3, I and J). PSA-FITC localized the shaft and frustules, whereas VFA-FITC and GS II-FITC did not bind to any diatom material. Stalks autofluoresced light blue under 360-nm excitation, and upon addition of DAPI, the nuclei, stalks, and frustules fluoresced intensely blue (Fig. 3F). Tinopal labeled pads, collars, and rapheless valves, whereas Ruthenium red stained the core of the shaft more intensely than the outer layers. No ECM was found to be birefringent.

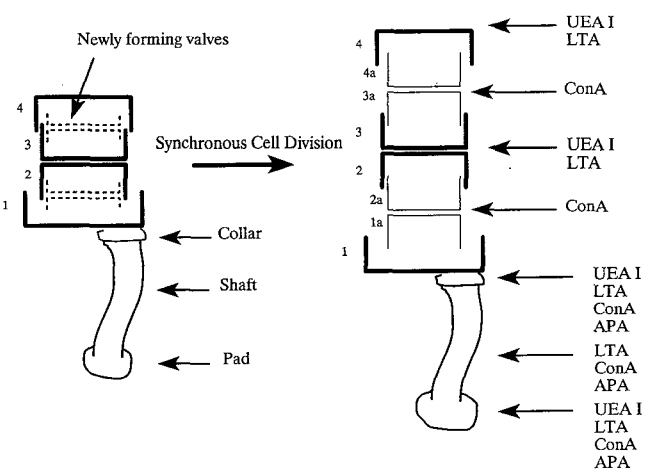

Figure 2. Summary of labeling patterns of UEA I-FITC, LTA-FITC, and ConA-FITC *A. longipes* frustules and stalks. Synchronous cell division results in stacks of cells with alternating junctions of immature valves (indicated by thin lines) and mature valves (indicated by thick lines).

Amino acid profiles for hydrolyzed MIS show Ala (17% [mol%]), Val (13%), Gly (13%), Ser (13%), and Asp/Asn (13%) as the major amino acid constituents of proteins from *A. longipes* ECM. A modified amino acid was also detected as a major component, but could not be identified by this protocol; Glu and Asp could not be differentiated from Gln and Asn, respectively.

C. cistula: Freshwater Stalk Former

C. cistula becomes motile immediately after initial attachment. Cells demonstrate a raphe-substratum interface orientation during motility. Eventually, cell motility ceases and basal pads are formed at one apical pore field. The pads are separated from the cell by the production of shafts. Shafts elongate in a spring-like circular spiral until stalks >500 μm in length are obtained. Cell division results in Y-branched shafts. Sexual reproduction of *C. cistula* was never observed in our cultures.

No evidence of uronosyl residues in polymers isolated from *C. cistula* was revealed by carbazole assay, monosaccharide analysis with CMC prereduction, or methylation analysis. Galactosyl (3,4,6-; 4,6-; 3,4-; and 4-linked/substituted) and xylosyl (*t*- and $4_f/5_p$-linked/substituted) residues were the major substituents of *C. cistula* MIS (Table I). The 0.2 M EDTA-soluble fraction consisted mostly of galactosyl (4-; 4,6-; and 3,4-linked/substituted) and xylosyl (*t*-; $4_f/5_p$-; and 3_p-linked/substituted) residues (Table I). Sulfate analysis indicated 15% sulfate in the *C. cistula* stalks. IR analysis of MIS revealed absorbances between 805 and 850 cm^{-1} and at approximately 1240 cm^{-1}, which correspond to those reported for sulfated galactans (Craigie and Leigh, 1978).

Lectin labeling patterns are summarized in Table II. APA-FITC labeled frustules and stalks (Fig. 3L), ConA-FITC labeled frustules (Fig. 3M), and UEA I-FITC labeled nonstalk ECM associated with the apical pore fields (Fig. 3N). No labeling of cells or ECM was observed using PSA-, VFA-, or GS II-FITC. Stalks did not autofluoresce when excited at 360 nm, and upon addition of DAPI, stalks fluoresced yellow and nuclei fluoresced blue (Fig. 3K; Table II). Tinopal stained only nonstalk mucilage associated with the apical pore field, Ruthenium red stained only the capsular material, and ECM was not birefringent.

Approximately 1.5% of MIS was protein, and amino acid analysis revealed six major amino acids: Gly (23% [mol%]), Glu/Gln (18%), Arg (9%), Ala (8%), Asp/Asn (8%), and Ser (7%).

Table II. *Lectin localization and staining patterns for diatom adhesives*

Diatom cell/adhesive staining patterns with FITC-conjugated lectin, DAPI, Tinopal, and Ruthenium red. Controls consisted of preabsorption of lectins by fucoidan, cellulose, or mannan, or by competing off bound lectin with the appropriate monosaccharide.

Application	Specific[a]	Control	*A. longipes*	*C. cistula*	*A. coffeaeformis*
APA-FITC (*A. precatorius*)	D-Gal	D-Gal	-shaft -pad -collar -gamate encapsulating matrix	-shaft -frustule -raphe	-capsule
LTA-FITC (*L. tetragonolobus*)	α(*t*)-L-Fuc	Fucoidan	-shaft -pad -collar -between stacked cells	No labeling	No labeling
UEA I-FITC (*U. europaeus*)	α(1,2)-L-Fuc	Fucoidan	-pad -collar -between stacked cells -polar nodule region	-mucilage associated with apical pore field	No labeling
ConA-FITC (*C. ensiformis*)	α-D-Man α-D-Glc	Cellulose Mannan	-shaft -pad -collar -immature valve	-frustule	-between cells -organic sheath
PSA-FITC (*P. sativum*)	D-Man	Mannan	-shaft -frustule	No labeling	
VFA-FITC (*V. faba*)	Man Glc GlcNAc	Cellulose Mannan	No labeling	No labeling	No labeling
GS II-FITC (*G. simplicifolia*)	α(*t*)-GlcNAc β(*t*)-GlcNAc	Chitin	No labeling	No labeling	No labeling
DAPI	DNA Sulfated dextran Negatively charged polyelectrolytes (blue) Polyphosphate unbound DAPI (yellow)		-shaft -pad -collar -frustule -nucleus (blue)	-nucleus (blue) -shaft -frustule (yellow)	-nucleus -frustule (blue)
Autofluorescence (360 nm)			-shaft (light blue)	None	None
Birefringent		Crystalline cellulose	No	No	No
Ruthenium red	Anionic carbohydrates		-capsule -pad -shaft (core) -collar	-capsule	-capsule
Tinopal	β-Glycan	Cellulose	-pad -collar -rapheless valve	-mucilage associated with apical pore field	-capsule -frustule

[a] Lectin specificities were obtained from EY Laboratories, Inc. (San Mateo, CA).

C. mexicana: Freshwater Stalk Former

Monosaccharide analysis revealed galactosyl (4-Gal) and xylosyl ($4_f/5_p$-Xyl) units in the MIS of *C. mexicana* (Table I). Uronosyl units were not a major component of *C. mexicana* polymers. IR analysis of MIS revealed absorbances between 805 and 850 cm^{-1} and approximately 1240 cm^{-1} for ester sulfate (Craigie and Leigh, 1978).

A. coffeaeformis: Marine Capsule Producer

Mucilage capsules mechanically isolated from *A. coffeaeformis* contain a substantial amount of GlcUA, Glc, Fuc, Gal, Man, Xyl, and Rha in near equal proportions (Table I). Methylation analysis yielded considerable quantities of *t*- and 4-GlcUA, although uronic acid was not a major component (approximately 7%) in monosaccharide determinations. Sulfate and protein contents of mechanically isolated capsules were estimated to be 13 and 6%, respectively.

The FITC-conjugated lectins LTA and UEA I did not bind to the frustules or mucilage capsules. APA-FITC lectin bound to a loosely associated capsule component, whereas ConA-FITC bound to organic sheaths closely associated with cells (Table II) and between recently divided cells. No localization of cells or ECM was detected using PSA-, VFA-, or GS II-FITC.

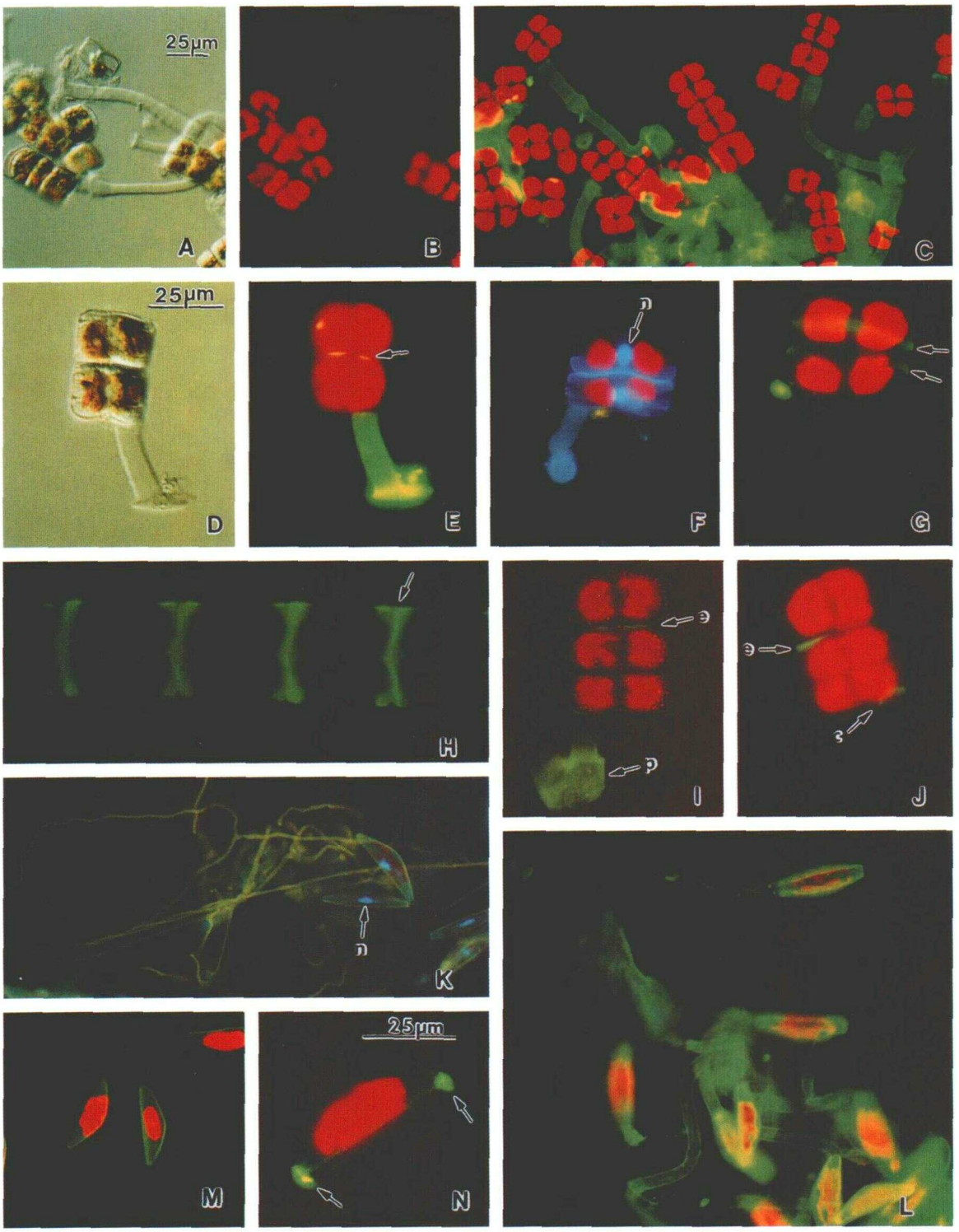

Figure 3. FITC-lectin and DAPI localization of ECM of *A. longipes* and *C. cistula*. A to E, Localization of Fuc units in *A. longipes* ECM with LTA-FITC using epifluorescence correlated with DIC microscopy (A) and corresponding fluorescence image (B) produced following labeling with LTA-FITC preabsorbed with fucoidan. C, Stalks labeled with LTA-FITC. D, DIC microscopy and E, corresponding epifluorescence of LTA-FITC-labeled extracellular polymers between two mature frustules (arrow). F, DAPI-labeled valves, stalk, and nuclei (n) of *A. longipes*. G, Polymers in *A. longipes* stalk and immature valves (arrows) labeled by ConA-FITC. H, Within a stack of cells, ConA-FITC binds immature valve junctions between every other cell. I and J, UEA I-FITC-labeled *A. longipes* pads (p), collars (c), and ECM between mature valves (e). K, DAPI localized in nuclei (n) of *C. cistula*. Stalks and frustules exhibit a yellow fluorescence in the presence of DAPI. L, *C. cistula* stalks and frustules labeled with APA-FITC. M, ConA-FITC localized in frustules of *C. cistula*. N, ECM associated with the apical pore field of *C. cistula* (arrows) was labeled with UEA I-FITC. Scale for E to J and L is as in D; scale for B, C, K, and M is as in A.

Capsular material did not autofluoresce when exposed to UV (360 nm); however, frustules and nuclei fluoresced blue upon addition of DAPI. Tinopal stained capsules and frustules, Ruthenium red stained capsules only, and ECM polymers were not birefringent.

DISCUSSION

A. longipes

Alcian staining and EM techniques indicated that the shaft is made up of four regions, an inner sulfated core with polymers organized perpendicular to the axis of shaft elongation, and three outer layers with a predominance of uronosyl residues and oriented parallel to the axis of shaft elongation (Daniel et al., 1987; Wang et al., 1997). The varying solubility of polysaccharides in CPC, monosaccharide and linkage analysis of the adhesive fractions, cytochemical staining, and lectin-FITC labeling of shafts indicate that the shaft core consists of polymers rich in sulfated galactosyl (2,3- and/or 3,6-Gal) residues, whereas those in the outer layers are composed primarily of *t*- and 2-GlcUA, *t*-Fuc, D-Gal, and D-Man units (Tables I and II). Our finding of 5% sulfate, some of which is present as ester sulfate as indicated by IR analysis, correlates with recent scanning electron microscopy-energy dispersive x-ray analysis indicating sulfur as an important elemental component of *A. longipes* stalks (Novarino, 1993). The anionic nature of the adhesive polymers may be responsible for the unexpected results observed with DAPI labeling (Fig. 3F). The mechanism of DAPI labeling of extracellular structures is not known, although it has been reported that negatively charged polyelectrolytes (Tijssen et al., 1982) and dextran sulfate (a sulfated glucan) complex and fluoresce with DAPI, yielding a blue emission.

Based on microscopical observations, cytochemical staining, and lectin labeling, pads and collars are composed of similar adhesive material. As shaft synthesis moves the cell away from the substratum, part of the pad remains attached to the bottom of the frustule, creating a collar around the shaft in the terminal nodule region (Daniel et al., 1987; Wang et al., 1997). Pads and collars were labeled by UEA I-, LTA-, and APA-FITC, and Alcian staining indicated carboxylated polymers in the collars and at the sites of attachment (Daniel et al., 1987). These results, coupled with linkage/substitution analysis, indicate that the polymers making up the pads and collars are rich in GlcUA, D-Gal, 2-, and *t*-Fuc residues (Tables I and II).

That *A. longipes* polymers are organized and assembled into networks by phenolic cross-linking components is suggested by several results: (a) the blue autofluorescence of the stalks when excited by UV light >360 nm; (b) Johnson et al. (1995) have characterized a bromide dependence for stalk synthesis in *A. longipes* and also found that iodide inhibits stalk production; and (c) V. Vreeland (personal communication) found preliminary cytochemical evidence for peroxidase activity within intracellular vesicles in *A. longipes* cells. Phenolic compounds such as dityrosine, ferulic acid, feruloyl esters, caffeic acid, and sinapic acid are known to fluoresce blue when exposed to 366-nm UV light (Fry, 1995). Dityrosine- and isodityrosine-containing glycoproteins have been identified in the cell walls of the green alga *Chlamydomonas* (Waffenschmidt et al., 1993), and polyphenolics are involved in cross-linking extracellular polymers of *Fucus* embryos via a bromide-/vanadate-dependent bromoperoxidase (Vreeland and Epstein, 1995). We are currently investigating the possibility of a bromide-dependent, peroxidase-mediated phenolic cross-linking of extracellular adhesive polymers of *A. longipes*.

The shift from cell motility to pad production and, finally, to shaft production and elongation may be mediated through multiple polymer cross-linking processes. When pads are first forming, the cells make jerking movements as if still attempting to move. After the jerking ceases and the pad stops growing, a shaft begins to appear between the cell and pad. The newly synthesized shaft material appears to undergo extracellular modification, since regions near the raphe swell when extracted with hot water and shrink considerably more than the rest of the stalk when dried, which may be due to less extensive cross-linking of newly extruded polymers.

A. longipes cells adhere to the substratum by either passive or active means; passive attachment involves existing polymers and is the most rapid means of attachment (Wang et al., 1997). Hydrophobic polymers are known to play an important role in the nonspecific adhesion and colonization of many bacteria and cyanobacteria (Fattom and Shilo, 1984). The hydrophobic nature of *A. longipes* cells and stalks may be due in part to the hydrophobic $-CH_3$ group of the fucosyl residues, which were identified as a major sugar component of the adhesive and were localized in the stalks, pads, and collars by UEA I- and LTA-FITC lectins (Tables I and II; Fig. 3, C, E, I, and J). Monosaccharide analysis also identified rhamnosyl and an unidentified methylated hexosyl residue as minor components (Table I). Polysaccharides lacking hydrophobic groups may also show hydrophobic properties by forming "inclusion complexes" by orienting several -H of rotatable C-H positions to point in the same direction, creating a hydrophobic region to one side of the chain (Christensen, 1989).

Active attachment is associated with synthesis of ECM and usually occurs immediately after passive attachment, making a stronger adhesive bond (Wang et al., 1997). One form of active attachment, which generally results in a firm raphid valve-surface association, is propagated by the generation of *t*- and 2-Fuc containing adhesives expelled through the raphe, which are involved in cell motility as described above. Cell motility ceases as pad production takes over, forming the first permanent adhesive structure.

Wang et al. (1997) observed that under optimal conditions cell division occurred synchronously, resulting in stacks of cell filaments with a pattern of cell junctions alternating between two immature valves and two mature valves (Fig. 3). Dispersion of cells from stacks occurred by dissociation into two cell units and, finally, into individual cells, with cells separating only at mature valve interfaces. When cell filaments were labeled with UEA I-, LTA-, and ConA-FITC, an alternating pattern of localization emerged. ConA-FITC labeled only the immature valves (Fig. 3, G and H), which

were tightly associated with one another and lacked any observable pad or stalk-like material between the valves. Mannosyl and/or glucosyl residues, which predominate in the insoluble residue fraction (which was chiefly frustules) (Table I), are the likely binding sites. UEA I- and LTA-FITC labeling of *t*- and 2-Fuc residues in extracellular material produced at one or both ends of mature valve interfaces (Fig. 3, E, I, and J; Table II) did not occur between firmly adhered immature valves, indicating that these residues are not required for cell-cell adhesion. However, UEA I- and LTA-FITC and Tinopal also labeled pads and saccharide between mature frustules at the onset of motility, demonstrating a chemical relationship between primary adhesive structures and polymers involved in cell motility.

C. cistula and *C. mexicana*

Microscopic observations of *C. cistula* and *C. mexicana* revealed motile cells coated by an organic sheath, which eventually produce one or two stalks from apical pore field(s). The stalk shaft was attached to the substrate by an apical pad, and collars were occasionally present. APA-FITC bound both stalks and organic sheaths, supporting chemical characterization indicating Gal as a major glycosyl component of the adhesive polymers (Table I; Fig. 3L). *C. cistula* adhesives are unique from those of *A. longipes* in that *C. cistula* stalks are made up almost entirely of a highly sulfated xylogalactan (Table I), lack any detectable uronic acid residues, do not have an organized substructure (such as shaft cores or multiple outer layers), and interact with DAPI to produce a yellow emission (Fig. 3K). EDTA and *trans*-1,2-diaminocyclohexane-*N,N,N',N'*-tetraacetic acid completely solubilized *C. cistula* stalks, indicating that the polymers may be assembled via a cation (Ca^{2+} and/or Mg^{2+})-mediated cross-linking.

Cells lacking stalks were often found to have mucilage associated with the apical pore fields at both ends of the cell, which was labeled by UEA I-FITC (Fig. 3N) and Tinopal. As in *A. longipes*, these two probes may localize a *t*-fucosyl residue containing a polymer involved in initial adhesion or motility. ConA-FITC localizes the frustules of *C. cistula* (Fig. 3M), revealing the presence of D-Man and/or D-Glc residues in the cell wall.

Stalk polymers of *C. cistula* and *C. mexicana* are similar to those reported for another freshwater diatom, *Gomphonema olivaceum* (Huntsman, 1966). As in *C. cistula*, *G. olivaceum* produces a sulfated xylogalactan that gels in the presence of Ca^{2+} and possesses some physical characteristics of the sulfated galactans of red algae (Huntsman and Sloneker, 1971). Protein may play a role in this gel formation, since gelling of *G. olivaceum* water-soluble stalk polymers was lost with trypsin digestion (Huntsman, 1966). Proteins and/or glycoproteins, such as the Ca^{2+} binding glycoproteins recently isolated from the marine diatom *Cylindrotheca olivaceum* (Kroger et al., 1995), may be involved in assembly and structural organization of freshwater diatom adhesives.

A. coffeaeformis

A. coffeaeformis adhered to surfaces via an organic sheath and was also surrounded by a much more loosely associated mucilaginous capsule. The capsule and organic sheath were differentially labeled by APA- and ConA-FITC, with APA-FITC localizing only the capsule and ConA-FITC labeling the tightly associated organic sheath of attached cells. ConA-FITC also localized the immature valves of *A. coffeaeformis*, providing evidence of D-Man and/or D-Glc residues. UEA I- and LTA-FITC did not bind *A. coffeaeformis* mucilage, indicating that the fucosyl units detected by monosaccharide and methylation analysis were unavailable.

As in *A. longipes*, *A. coffeaeformis* contains a substantial amount of GlcUA and sulfate in its adhesive polymers, and Daniel et al. (1980) provided evidence for carboxylated polymers at the site of attachment. Medcalf et al. (1981) also found evidence for sulfate and uronic acid, and identified 3- and 4-linked glucosyl, 3-linked xylosyl, and *t*- and 2-linked galactosyl as the major glycosyl residues in *A. coffeaeformis* adhesives. In addition, we were able to identify 4-, *t*-, and 2,4-linked glucuronosyl residues as major components and estimate a 7% uronic acid content.

There is evidence that cations may be involved in cross-bridging these adhesive polymers. Cooksey and Cooksey (1986) found that removal of Ca^{2+} by EGTA not only inhibited adhesion and motility in *A. coffeaeformis*, *Navicula*, *Nitzschia*, and *Troponeis* spp., but also caused "cohesive breaks" to occur in the mucilage. This suggests that adhesion to surfaces may be mediated by cation bridging of acidic polymers. However, in the freshwater diatoms *Craticula* spp. and *Nitzschia* spp., Cohn and Disparti (1994) found that motility was inhibited by EGTA, not by a lack of external Ca^{2+}, but that it may be affected by an internal Ca^{2+} reserve. Glycoprotein may also be important in the adhesion process of *A. coffeaeformis*, since Cooksey and Cooksey (1986) reported that glycoprotein synthesis is required for adhesion and motility.

CONCLUSIONS

All four diatoms produced adhesives directly involved in initial active attachment and cell motility. *t*-Fuc- and 2-Fuc-containing polymers appear to be involved in initial adhesion and cell motility in *A. longipes* and *C. cistula*. Glucuronosyl residues are indicated at the site of attachment for *A. coffeaeformis*, with a substantial amount of fucosyl and galactosyl (and possibly glucosyl) residues localized within the rest of the capsule. *A. longipes* shafts were made up of two distinct regions, a core containing sulfated galactosyl residues, and three outer layers rich in *t*- and 2-GlcUA and nonsulfated D-Gal and *t*-Fuc residues. *C. cistula* stalks consist of a sulfated xylogalactan cross-linked by Ca^{2+} and/or Mg^{2+} (with possible involvement of protein/glycoprotein). Cationic cross-bridging may also be involved in *A. longipes* and *A. coffeaeformis* adhesive assembly, although evidence suggests that *A. longipes* also possesses a peroxidase-mediated phenolic cross-linking mechanism. The models produced here provide a better understanding of how diatoms permanently adhere to surfaces in freshwater and marine environments.

ACKNOWLEDGMENTS

The authors thank Yan Wang and Jean-Claude Mollet for staining and microscopic observations and for their helpful discussions, Lisa Johnson and Jeff Robinson for assistance with lectin labeling, Karen Snitzer for assistance with carbohydrate analysis, Ian Marsden for NMR, Yalin Wu for amino acid analysis, and Ray Lewis and Dean DeNicola for their participation in culturing and subsequent isolation of diatom ECM.

Received August 16, 1996; accepted December 18, 1996.

LITERATURE CITED

Alberte RS, Snyder S, Zahuranec BJ, Whetstone M (1992) Biofouling research needs for the United States Navy: program history and goals. Biofouling **6:** 91–95

Barker SA, Hurst RE, Settine J, Fish FP, Settine RL (1984) Structural analysis of heparin by methylation and GLC-MS: preliminary results. Carbohydr Res **125:** 291–300

Bitter T, Muir HM (1962) A modified uronic acid carbazole reaction. Anal Biochem **4:** 330–334

Blakeney AB, Harris PJ, Henry RJ, Stone BA (1983) A simple and rapid preparation of alditol acetates for monosaccharide analysis. Carbohydr Res **113:** 291–299

Christensen BE (1989) The role of extracellular polysaccharides in biofilms. J Biotechnol **10:** 181–202

Cohn SA, Disparti NC (1994) Environmental factors influencing diatom cell motility. J Phycol **30:** 818–828

Cooksey KE, Cooksey B (1986) Adhesion of fouling diatoms to surfaces: some biochemistry. *In* LV Evans, KD Hoagland, eds, Algal Biofouling. Elsevier, Amsterdam, pp 41–53

Craigie JS, Leigh C (1978) Carrageenans and agars. *In* JA Hellebust, JS Craigie, eds, Handbook of Phycological Methods: Physiological and Biochemical Methods. Cambridge University Press, Cambridge, UK, pp 109–131

Craigie JS, Wen ZC, van der Meer JP (1984) Interspecific, intraspecific and nutritionally-determined variations in the composition of agars from *Gracilaria* spp. Bot Mar **27:** 55–61

Daniel GF, Chamberlain AHL, Jones EBG (1980) Ultrastructural observations on the marine fouling diatom *Amphora*. Helgol Wiss Meeresunters **34:** 123–149

Daniel GF, Chamberlain AHL, Jones EBG (1987) Cytochemical and electron microscopical observations on the adhesive materials of marine fouling diatoms. Br Phycol J **22:** 101–118

Darley WM (1977) Biochemical composition. *In* D Werner, ed, The Biology of Diatoms, Vol 13. University of California Press, Berkeley, pp 198–223

Darvill A, McNeil M, Albersheim P, Delmer D (1980) The primary cell walls of flowering plants. *In* NE Tolbert, ed, The Biochemistry of Plants, Vol I. Academic Press, New York, pp 91–162

Fattom A, Shilo M (1984) Hydrophobicity as an adhesion mechanism of benthic cyanobacteria. Appl Environ Microbiol **47:** 135–143

Fry SC (1995) Wall polymers: chemical characterisation. *In* M Wilkins, ed, The Growing Plant Cell Wall: Chemical and Metabolic Analysis. John Wiley & Sons, New York, pp 102–187

Guillard RRL (1975) Culture of phytoplankton for feeding marine invertebrates. *In* WL Smith, MH Chanley, eds, Culture of Marine Invertebrate Animals. Plenum, New York, pp 29–60

Harris PJ, Henry RJ, Blakeney AB, Stone BA (1984) An improved procedure for the methylation analysis of oligosaccharides and polysaccharides. Carbohydr Res **127:** 59–73

Hoagland KD, Rosowski JR, Gretz MR, Roemer SC (1993) Diatom extracellular polymeric substances: function, fine structure, chemistry, and physiology. J Phycol **29:** 537–566

Huntsman SA (1966) The stalk polysaccharide of the diatom *Gomphonema olivaceum*. PhD dissertation. Iowa State University, Ames, IA

Huntsman SA, Sloneker JH (1971) An exocellular polysaccharide from the diatom *Gomphonema olivaceum*. J Phycol **7:** 261–264

Jansson P, Kenne L, Leidgren H, Lindberg B, Lönngren J (1976) A Practical Guide to the Methylation Analysis of Carbohydrates. Chemical Communication No 8. Department of Organic Chemistry, Stockholm University, pp. 1–75

Johnson LM, Hoagland KD, Gretz MR (1995) Effects of bromide and iodide on stalk secretion in the biofouling diatom *Achnanthes longipes* (Bacillariophyceae). J Phycol **31:** 401–412

Kim J-B, Carpita NC (1992) Changes in esterification of the uronic acid groups of cell wall polysaccharides during elongation of maize coleoptiles. Plant Physiol **98:** 646–653

Kroger N, Bergsdorf C, Sumper M (1995) A new calcium binding glycoprotein family constitutes a major diatom cell wall component. EMBO J **13:** 4676–4683

Kvernheim AL (1987) Methylation analysis of polysaccharides with butyllithium in dimethyl sulfoxide. Acta Chem Scand **B41:** 150–152

Lowry OH, Rosebrough NJ, Farr AL, Randall RJ, Ricart G (1951) Protein measurement with the Folin phenol reagent. J Biol Chem **193:** 265–275

Medcalf DG, Brannon JH, Scott JR, Allan GG, Lewis J, Norris RE (1981) Polysaccharides from microscopic red algae and diatoms. Proc Int Seaweed Symp **8:** 582–588

Novarino G (1993) Presence of minerals in the mucilage stalk of the diatom *Achnanthes longipes*. Diatom Res **8:** 199–202

Paz Parente J, Cardon P, Leroy Y, Montreuil J, Fournet B (1985) A convenient method for methylation of glycoprotein glycans in small amounts by using lithium methylsulfinyl carbanion. Carbohydr Res **141:** 41–47

Pringsheim EG (1946) Pure Cultures of Algae. Cambridge University Press, London

Round FE, Crawford RM, Mann DG (1990) The Diatoms: Biology and Morphology of the Genera. Cambridge University Press, New York

Sloneker JH (1972) Gas-liquid chromatography of alditol acetates. *In* RL Whistler, JN Bemiller, eds, Methods in Carbohydrate Chemistry, Vol VI. Academic Press, New York, pp 20–24

Stevenson TT, Furneaux RH (1991) Chemical methods for the analysis of sulfated galactans from red algae. Carbohydr Res **210:** 277–298

Taylor RL, Conrad HE (1972) Stoichiometric depolymerization of polyuronides and glycosaminoglycuronans to monosaccharides following reduction of their carbodiimide-activated carboxyl groups. Biochemistry **11:** 1383–1389

Tijssen JPF, Beekes HW, Van Steveninck J (1982) Localization of polyphosphates in *Saccharomyces fragilis*, as revealed by 4′,6-diamidino-2-phenylindole fluorescence. Biochim Biophys Acta **721:** 394–398

Vreeland V, Epstein L (1995) Analysis of plant-substratum adhesives. *In* JF Jackson, HF Linskins, eds, Modern Methods of Plant Analysis: Plant Cell Wall Analysis, Vol 17. Springer-Verlag, Berlin

Waeghe TJ, Darvill AG, McNeil M, Albersheim P (1983) Determination, by methylation analysis, of the glycosyl-linkage compositions of microgram quantities of complex carbohydrates. Carbohydr Res **123:** 281–304

Waffenschmidt S, Woessner JP, Beer K, Goodenough UW (1993) Isodityrosine cross-linking mediates insolubilization of cell walls in *Chlamydomonas*. Plant Cell **5:** 809–820

Wang Y (1995) A study of adhesion mechanisms of the marine biofouling alga, *Achnanthes longipes* (Bacillariophyceae). Master's thesis. Michigan Technological University, Houghton

Wang Y, Lu J, Mollet J-C, Gretz MR, Hoagland KD (1997) Extracellular matrix assembly in diatoms (Bacillariophyceae). II. 2,6-Dichlorobenzonitrile inhibition of motility and stalk production in the marine diatom *Achnanthes longipes*. Plant Physiol **113:** 1071–1080

York WS, Darvill AG, McNeil M, Stevenson TT, Albersheim P (1985) Isolation and characterization of plant cell walls and cell wall components. Methods Enzymol **118:** 3–40